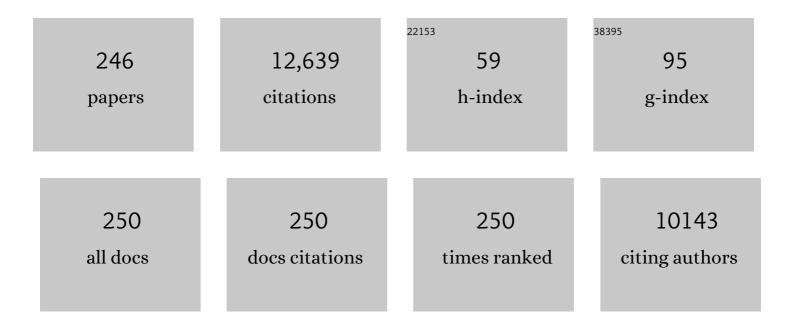
List of Publications by Year in descending order

Source: https://exaly.com/author-pdf/1929871/publications.pdf Version: 2024-02-01



FANC-RALL

#	Article	IF	CITATIONS
1	Generation of low-cadmium rice germplasms via knockout of OsLCD using CRISPR/Cas9. Journal of Environmental Sciences, 2023, 126, 138-152.	6.1	12
2	Unique feature of Fe-OM complexes for limiting Cd accumulation in grains by target-regulating gene expression in rice tissues. Journal of Hazardous Materials, 2022, 424, 127361.	12.4	9
3	Kinetics of antimony biogeochemical processes under pre-definite anaerobic and aerobic conditions in a paddy soil. Journal of Environmental Sciences, 2022, 113, 269-280.	6.1	11
4	Electron shuttle-induced oxidative transformation of arsenite on the surface of goethite and underlying mechanisms. Journal of Hazardous Materials, 2022, 425, 127780.	12.4	21
5	Sustainability assessment and carbon budget of chemical stabilization based multi-objective remediation of Cd contaminated paddy field. Science of the Total Environment, 2022, 819, 152022.	8.0	18
6	Bioavailability of antimony and arsenic in a flowering cabbage–soil system: Controlling factors and interactive effect. Science of the Total Environment, 2022, 815, 152920.	8.0	15
7	<i>Serratia</i> spp. Are Responsible for Nitrogen Fixation Fueled by As(III) Oxidation, a Novel Biogeochemical Process Identified in Mine Tailings. Environmental Science & amp; Technology, 2022, 56, 2033-2043.	10.0	46
8	Biogeochemical Fe(II) generators as a new strategy for limiting Cd uptake by rice and its implication for agricultural sustainability. Science of the Total Environment, 2022, 820, 153306.	8.0	20
9	Desulfurivibrio spp. mediate sulfur-oxidation coupled to Sb(V) reduction, a novel biogeochemical process. ISME Journal, 2022, 16, 1547-1556.	9.8	48
10	Foliar application of silica nanoparticles alleviates arsenic accumulation in rice grain: co-localization of silicon and arsenic in nodes. Environmental Science: Nano, 2022, 9, 1271-1281.	4.3	10
11	Silicon reduces the uptake of cadmium in hydroponically grown rice seedlings: why nanoscale silica is more effective than silicate. Environmental Science: Nano, 2022, 9, 1961-1973.	4.3	20
12	Source and Strategy of Iron Uptake by Rice Grown in Flooded and Drained Soils: Insights from Fe Isotope Fractionation and Gene Expression. Journal of Agricultural and Food Chemistry, 2022, 70, 2564-2573.	5.2	5
13	Facet-dependent Fe(II) redox chemistry on iron oxide for organic pollutant transformation and mechanisms. Water Research, 2022, 219, 118587.	11.3	11
14	Tetracycline-Induced Release and Oxidation of As(III) Coupled with Concomitant Ferrihydrite Transformation. Environmental Science & Technology, 2022, 56, 9453-9462.	10.0	12
15	Carbon-based strategy enables sustainable remediation of paddy soils in harmony with carbon neutrality. , 2022, 1, .		39
16	Simultaneous redox transformation and removal of Cr(â¥) and As(â¢) by polyethyleneimine modified magnetic mesoporous polydopamine nanocomposite: Insights into synergistic effects and mechanisms. Journal of Hazardous Materials, 2022, 439, 129581.	12.4	12
17	Impact of sulfate and iron oxide on bacterial community dynamics in paddy soil under alternate watering conditions. Journal of Hazardous Materials, 2021, 408, 124417.	12.4	23
18	Quinone-mediated dissimilatory iron reduction of hematite: Interfacial reactions on exposed {0 0 1} and {1 0 0} facets. Journal of Colloid and Interface Science, 2021, 583, 544-552.	9.4	21

#	Article	IF	CITATIONS
19	Multiple effects of nitrate amendment on the transport, transformation and bioavailability of antimony in a paddy soil-rice plant system. Journal of Environmental Sciences, 2021, 100, 90-98.	6.1	13
20	Fe(II)-induced transformation of iron minerals in soil ferromanganese nodules. Chemical Geology, 2021, 559, 119901.	3.3	10
21	Effect of riboflavin on active bacterial communities and arsenic-respiring gene and bacteria in arsenic-contaminated paddy soil. Geoderma, 2021, 382, 114706.	5.1	12
22	AÂhighlyÂporousÂanimalÂbone-derivedÂchar with a superiority of promoting nZVI for Cr(VI) sequestration in agricultural soils. Journal of Environmental Sciences, 2021, 104, 27-39.	6.1	47
23	Development of a new framework to estimate the environmental risk of heavy metal(loid)s focusing on the spatial heterogeneity of the industrial layout. Environment International, 2021, 147, 106315.	10.0	16
24	The overlooked role of carbonaceous supports in enhancing arsenite oxidation and removal by nZVI: Surface area versus electrochemical property. Chemical Engineering Journal, 2021, 406, 126851.	12.7	68
25	New insights into stoichiometric efficiency and synergistic mechanism of persulfate activation by zero-valent bimetal (Iron/Copper) for organic pollutant degradation. Journal of Hazardous Materials, 2021, 403, 123669.	12.4	59
26	Rapid and efficient removal of Cr( <scp>vi</scp> ) by a core–shell magnetic mesoporous polydopamine nanocomposite: roles of the mesoporous structure and redox-active functional groups. Journal of Materials Chemistry A, 2021, 9, 13306-13319.	10.3	61
27	Microaerophilic Oxidation of Fe(II) Coupled with Simultaneous Carbon Fixation and As(III) Oxidation and Sequestration in Karstic Paddy Soil. Environmental Science & amp; Technology, 2021, 55, 3634-3644.	10.0	29
28	Bacteria responsible for antimonite oxidation in antimony-contaminated soil revealed by DNA-SIP coupled to metagenomics. FEMS Microbiology Ecology, 2021, 97, .	2.7	13
29	Co-Cropping Indian Mustard and Silage Maize for Phytoremediation of a Cadmium-Contaminated Acid Paddy Soil Amended with Peat. Toxics, 2021, 9, 91.	3.7	9
30	Solar-driven, self-sustainable electrolysis for treating eutrophic river water: Intensified nutrient removal and reshaped microbial communities. Science of the Total Environment, 2021, 764, 144293.	8.0	6
31	Impacts of Redox Conditions on Arsenic and Antimony Transformation in Paddy Soil: Kinetics and Functional Bacteria. Bulletin of Environmental Contamination and Toxicology, 2021, 107, 1121-1127.	2.7	1
32	Bacteria responsible for nitrate-dependent antimonite oxidation in antimony-contaminated paddy soil revealed by the combination of DNA-SIP and metagenomics. Soil Biology and Biochemistry, 2021, 156, 108194.	8.8	25
33	Fulvic Acid-Mediated Interfacial Reactions on Exposed Hematite Facets during Dissimilatory Iron Reduction. Langmuir, 2021, 37, 6139-6150.	3.5	16
34	New insight into iron biogeochemical cycling in soil-rice plant system using iron isotope fractionation. Fundamental Research, 2021, 1, 277-284.	3.3	5
35	Different effects of foliar application of silica sol on arsenic translocation in rice under low and high arsenite stress. Journal of Environmental Sciences, 2021, 105, 22-32.	6.1	11
36	Integrated Life Cycle Assessment for Sustainable Remediation of Contaminated Agricultural Soil in China. Environmental Science & Technology, 2021, 55, 12032-12042.	10.0	62

#	Article	IF	CITATIONS
37	Distinct biofilm formation regulated by different culture media: Implications to electricity generation. Bioelectrochemistry, 2021, 140, 107826.	4.6	4
38	Chemodenitrification by Fe(II) and nitrite: Effects of temperature and dual N O isotope fractionation. Chemical Geology, 2021, 575, 120258.	3.3	16
39	Water Management Alters Cadmium Isotope Fractionation between Shoots and Nodes/Leaves in a Soil-Rice System. Environmental Science & Technology, 2021, 55, 12902-12913.	10.0	12
40	Identification of Antimonate Reducing Bacteria and Their Potential Metabolic Traits by the Combination of Stable Isotope Probing and Metagenomic-Pangenomic Analysis. Environmental Science & Technology, 2021, 55, 13902-13912.	10.0	22
41	Modelling evaluation of key cadmium transformation processes in acid paddy soil under alternating redox conditions. Chemical Geology, 2021, 581, 120409.	3.3	28
42	Comparative physiological and transcriptomic analyses illuminate common mechanisms by which silicon alleviates cadmium and arsenic toxicity in rice seedlings. Journal of Environmental Sciences, 2021, 109, 88-101.	6.1	36
43	New Arsenite Oxidase Gene (aioA) PCR Primers for Assessing Arsenite-Oxidizer Diversity in the Environment Using High-Throughput Sequencing. Frontiers in Microbiology, 2021, 12, 691913.	3.5	2
44	Anaerobic ammonium oxidation is a major N-sink in aquifer systems around the world. ISME Journal, 2020, 14, 151-163.	9.8	54
45	Development of a new framework to identify pathways from socioeconomic development to environmental pollution. Journal of Cleaner Production, 2020, 253, 119962.	9.3	24
46	Silica nanoparticles inhibit arsenic uptake into rice suspension cells <i>via</i> improving pectin synthesis and the mechanical force of the cell wall. Environmental Science: Nano, 2020, 7, 162-171.	4.3	98
47	Kinetics of As(V) and carbon sequestration during Fe(II)-induced transformation of ferrihydrite-As(V)-fulvic acid coprecipitates. Geochimica Et Cosmochimica Acta, 2020, 272, 160-176.	3.9	63
48	Behaviors of heavy metal(loid)s in a cocontaminated alkaline paddy soil throughout the growth period of rice. Science of the Total Environment, 2020, 716, 136204.	8.0	17
49	Acid-base buffering characteristics of non-calcareous soils: Correlation with physicochemical properties and surface complexation constants. Geoderma, 2020, 360, 114005.	5.1	33
50	Bacterial Communities and Functional Genes Stimulated During Anaerobic Arsenite Oxidation and Nitrate Reduction in a Paddy Soil. Environmental Science & Technology, 2020, 54, 2172-2181.	10.0	62
51	Interactive effects of multiple heavy metal(loid)s on their bioavailability in cocontaminated paddy soils in a large region. Science of the Total Environment, 2020, 708, 135126.	8.0	51
52	Extracellular Electron Shuttling Mediated by Soluble <i>c</i> -Type Cytochromes Produced by <i>Shewanella oneidensis</i> MR-1. Environmental Science & Technology, 2020, 54, 10577-10587.	10.0	61
53	Investigation of the Ecological Roles of Putative Keystone Taxa during Tailing Revegetation. Environmental Science & Technology, 2020, 54, 11258-11270.	10.0	62
54	Facet-dependent reductive dissolution of hematite nanoparticles by <i>Shewanella putrefaciens</i> CN-32. Environmental Science: Nano, 2020, 7, 2522-2531.	4.3	21

#	Article	IF	CITATIONS
55	Zinc isotope revealing zinc's sources and transport processes in karst region. Science of the Total Environment, 2020, 724, 138191.	8.0	34
56	Quantifying Microbially Mediated Kinetics of Ferrihydrite Transformation and Arsenic Reduction: Role of the Arsenate-Reducing Gene Expression Pattern. Environmental Science & Technology, 2020, 54, 6621-6631.	10.0	45
57	Characterization of Nitrate-Dependent As(III)-Oxidizing Communities in Arsenic-Contaminated Soil and Investigation of Their Metabolic Potentials by the Combination of DNA-Stable Isotope Probing and Metagenomics. Environmental Science & Technology, 2020, 54, 7366-7377.	10.0	82
58	Dual nitrogen-oxygen isotopic analysis and kinetic model for enzymatic nitrate reduction coupled with Fe(II) oxidation by Pseudogulbenkiania sp. strain 2002. Chemical Geology, 2020, 534, 119456.	3.3	19
59	Chemodenitrification by Fe(II) and nitrite: pH effect, mineralization and kinetic modeling. Chemical Geology, 2020, 541, 119586.	3.3	22
60	Community dynamics of As(V)-reducing and As(III)-oxidizing genes during a wet–dry cycle in paddy soil amended with organic matter, gypsum, or iron oxide. Journal of Hazardous Materials, 2020, 393, 122485.	12.4	26
61	Chemolithoautotropic Diazotrophy Dominates the Nitrogen Fixation Process in Mine Tailings. Environmental Science & Technology, 2020, 54, 6082-6093.	10.0	63
62	Conduction Band of Hematite Can Mediate Cytochrome Reduction by Fe(II) under Dark and Anoxic Conditions. Environmental Science & Technology, 2020, 54, 4810-4819.	10.0	52
63	Spatiotemporal patterns and drivers of soil contamination with heavy metals during an intensive urbanization period (1989–2018) in southern China. Environmental Pollution, 2020, 260, 114075.	7.5	81
64	Biochar's stability and effect on the content, composition and turnover of soil organic carbon. Geoderma, 2020, 364, 114184.	5.1	154
65	Application of Hydrochar Altered Soil Microbial Community Composition and the Molecular Structure of Native Soil Organic Carbon in a Paddy Soil. Environmental Science & Technology, 2020, 54, 2715-2725.	10.0	111
66	Enhanced Current Production by Exogenous Electron Mediators via Synergy of Promoting Biofilm Formation and the Electron Shuttling Process. Environmental Science & Technology, 2020, 54, 7217-7225.	10.0	63
67	Simultaneous removal of Cd(II) and As(III) by graphene-like biochar-supported zero-valent iron from irrigation waters under aerobic conditions: Synergistic effects and mechanisms. Journal of Hazardous Materials, 2020, 395, 122623.	12.4	174
68	Dynamics of gene expression associated with arsenic uptake and transport in rice during the whole growth period. BMC Plant Biology, 2020, 20, 133.	3.6	26
69	Microbially mediated nitrate-reducing Fe(II) oxidation: Quantification of chemodenitrification and biological reactions. Geochimica Et Cosmochimica Acta, 2019, 256, 97-115.	3.9	83
70	The applicability of biochar and zero-valent iron for the mitigation of arsenic and cadmium contamination in an alkaline paddy soil. Biochar, 2019, 1, 203-212.	12.6	45
71	lsotopic fingerprints indicate distinct strategies of Fe uptake in rice. Chemical Geology, 2019, 524, 323-328.	3.3	15
72	Biological Fe(II) and As(III) oxidation immobilizes arsenic in micro-oxic environments. Geochimica Et Cosmochimica Acta, 2019, 265, 96-108.	3.9	44

#	Article	IF	CITATIONS
73	Oxidation and removal of As( <scp>iii</scp> ) from soil using novel magnetic nanocomposite derived from biomass waste. Environmental Science: Nano, 2019, 6, 478-488.	4.3	52
74	Enhanced debromination of tetrabromobisphoenol a by zero-valent copper-nanoparticle-modified green rusts. Environmental Science: Nano, 2019, 6, 970-980.	4.3	20
75	Coupled Kinetics Model for Microbially Mediated Arsenic Reduction and Adsorption/Desorption on Iron Oxides: Role of Arsenic Desorption Induced by Microbes. Environmental Science & Technology, 2019, 53, 8892-8902.	10.0	30
76	A paddy field study of arsenic and cadmium pollution control by using iron-modified biochar and silica sol together. Environmental Science and Pollution Research, 2019, 26, 24979-24987.	5.3	46
77	Cadmium solubility in paddy soil amended with organic matter, sulfate, and iron oxide in alternative watering conditions. Journal of Hazardous Materials, 2019, 378, 120672.	12.4	83
78	Using sequential extraction and DGT techniques to assess the efficacy of plant- and manure-derived hydrochar and pyrochar for alleviating the bioavailability of Cd in soils. Science of the Total Environment, 2019, 678, 543-550.	8.0	39
79	Effects of Rare Earth Elements' Physicochemical Properties on Their Stabilization during the Fe(II)aq-induced Phase Transformation of Ferrihydrite. ACS Earth and Space Chemistry, 2019, 3, 895-904.	2.7	12
80	Stabilization of Cd 2+ /Cr 3+ During Aqueous Fe(II)â€Induced Recrystallization of Alâ€Substituted Goethite. Soil Science Society of America Journal, 2019, 83, 483-491.	2.2	5
81	Bacterial response to antimony and arsenic contamination in rice paddies during different flooding conditions. Science of the Total Environment, 2019, 675, 273-285.	8.0	47
82	Effect of Degree of Silicification on Silica/Silicic Acid Binding Cd(II) and Its Mechanism. Journal of Physical Chemistry A, 2019, 123, 3718-3727.	2.5	12
83	Influence of Incubation Temperature on 9,10-Anthraquinone-2-Sulfonate (AQS)-Mediated Extracellular Electron Transfer. Frontiers in Microbiology, 2019, 10, 464.	3.5	11
84	Quantifying Redox Dynamics of c-Type Cytochromes in a Living Cell Suspension of Dissimilatory Metal-reducing Bacteria. Analytical Sciences, 2019, 35, 315-321.	1.6	12
85	Microaerobic Fe(II) oxidation coupled to carbon assimilation processes driven by microbes from paddy soil. Science China Earth Sciences, 2019, 62, 1719-1729.	5.2	21
86	Ligand mediated reduction of c-type cytochromes by Fe(II): Kinetic and mechanistic insights. Chemical Geology, 2019, 513, 23-31.	3.3	11
87	Microbially mediated coupling of nitrate reduction and Fe(II) oxidation under anoxic conditions. FEMS Microbiology Ecology, 2019, 95, .	2.7	57
88	Determination of the Redox Potentials of Solution and Solid Surface of Fe(II) Associated with Iron Oxyhydroxides. ACS Earth and Space Chemistry, 2019, 3, 711-717.	2.7	20
89	Humic Substances Facilitate Arsenic Reduction and Release in Flooded Paddy Soil. Environmental Science & Technology, 2019, 53, 5034-5042.	10.0	121
90	A transcriptomic (RNA-seq) analysis of genes responsive to both cadmium and arsenic stress in rice root. Science of the Total Environment, 2019, 666, 445-460.	8.0	67

#	Article	IF	CITATIONS
91	Physiological and Genomic Characterization of a Nitrate-Reducing Fe(II)-Oxidizing Bacterium Isolated from Paddy Soil. Geomicrobiology Journal, 2019, 36, 433-442.	2.0	9
92	Iron Redox Chemistry and Its Environmental Impact: A Virtual Special Issue. ACS Earth and Space Chemistry, 2019, 3, 2374-2375.	2.7	5
93	Arsenic contamination influences microbial community structure and putative arsenic metabolism gene abundance in iron plaque on paddy rice root. Science of the Total Environment, 2019, 649, 405-412.	8.0	48
94	Enhanced immobilization of arsenic and cadmium in a paddy soil by combined applications of woody peat and Fe(NO3)3: Possible mechanisms and environmental implications. Science of the Total Environment, 2019, 649, 535-543.	8.0	68
95	The translocation of antimony in soil-rice system with comparisons to arsenic: Alleviation of their accumulation in rice by simultaneous use of Fe(II) and NO3â°. Science of the Total Environment, 2019, 650, 633-641.	8.0	43
96	Mitigation of soil acidification through changes in soil mineralogy due to long-term fertilization in southern China. Catena, 2019, 174, 227-234.	5.0	40
97	Enhanced reduction of organic pollutants by Fe/Cu@Pd ternary metallic nanoparticles under aerobic conditions: Batch and membrane reactor studies. Chemical Engineering Journal, 2019, 360, 180-189.	12.7	31
98	Resuscitation of anammox bacteria after >10,000 years of dormancy. ISME Journal, 2019, 13, 1098-1109.	9.8	51
99	Dependence of Secondary Mineral Formation on Fe(II) Production from Ferrihydrite Reduction by <i>Shewanella oneidensis</i> MR-1. ACS Earth and Space Chemistry, 2018, 2, 399-409.	2.7	60
100	The effect of electron donors on the dechlorination of pentachlorophenol (PCP) and prokaryotic diversity in paddy soil. European Journal of Soil Biology, 2018, 86, 8-15.	3.2	16
101	The influence of Si(iv) on the reactivity of [î€,Fe(iii)]/[î€,Fe(ii)] couples for 2-nitrophenol reduction in γ-Al2O3 suspensions. RSC Advances, 2018, 8, 7465-7472.	3.6	1
102	Effects of Simultaneous Application of Ferrous Iron and Nitrate on Arsenic Accumulation in Rice Grown in Contaminated Paddy Soil. ACS Earth and Space Chemistry, 2018, 2, 103-111.	2.7	42
103	Rapid estimation of microbial biomass in acid red soils with and without substrate incorporation. Journal of Soils and Sediments, 2018, 18, 2904-2913.	3.0	1
104	Cadmium accumulation in edible flowering cabbages in the Pearl River Delta, China: Critical soil factors and enrichment models. Environmental Pollution, 2018, 233, 880-888.	7.5	35
105	Transcriptional Activity of Arsenic-Reducing Bacteria and Genes Regulated by Lactate and Biochar during Arsenic Transformation in Flooded Paddy Soil. Environmental Science & Technology, 2018, 52, 61-70.	10.0	105
106	Simultaneous alleviation of cadmium and arsenic accumulation in rice by applying zero-valent iron and biochar to contaminated paddy soils. Chemosphere, 2018, 195, 260-271.	8.2	281
107	Fe(II) oxidation and nitrate reduction by a denitrifying bacterium, Pseudomonas stutzeri LS-2, isolated from paddy soil. Journal of Soils and Sediments, 2018, 18, 1668-1678.	3.0	25
108	Biological and chemical processes of microbially mediated nitrate-reducing Fe(II) oxidation by Pseudogulbenkiania sp. strain 2002. Chemical Geology, 2018, 476, 59-69.	3.3	62

#	Article	IF	CITATIONS
109	Roles of different active metal-reducing bacteria in arsenic release from arsenic-contaminated paddy soil amended with biochar. Journal of Hazardous Materials, 2018, 344, 958-967.	12.4	123
110	Variable charges of a red soil from different depths: Acid-base buffer capacity and surface complexation model. Applied Clay Science, 2018, 159, 107-115.	5.2	24
111	Rhizosphere Microbial Response to Multiple Metal(loid)s in Different Contaminated Arable Soils Indicates Crop-Specific Metal-Microbe Interactions. Applied and Environmental Microbiology, 2018, 84,	3.1	47
112	Bacterial Survival Strategies in an Alkaline Tailing Site and the Physiological Mechanisms of Dominant Phylotypes As Revealed by Metagenomic Analyses. Environmental Science & Technology, 2018, 52, 13370-13380.	10.0	112
113	Cr Release from Cr-Substituted Goethite during Aqueous Fe(II)-Induced Recrystallization. Minerals (Basel, Switzerland), 2018, 8, 367.	2.0	12
114	Sustainable Electron Shuttling Processes Mediated by <i>Inâ€Situâ€</i> Deposited Phenoxazine. ChemElectroChem, 2018, 5, 2171-2175.	3.4	17
115	Contrasting Mg isotopic compositions between Fe-Mn nodules and surrounding soils: Accumulation of light Mg isotopes by Mg-depleted clay minerals and Fe oxides. Geochimica Et Cosmochimica Acta, 2018, 237, 205-222.	3.9	50
116	A causation-based method developed for an integrated risk assessment of heavy metals in soil. Science of the Total Environment, 2018, 642, 1396-1405.	8.0	12
117	Variations in grain cadmium and arsenic concentrations and screening for stable low-accumulating rice cultivars from multi-environment trials. Science of the Total Environment, 2018, 643, 1314-1324.	8.0	60
118	Attribution of Soil Acidification in a Largeâ€6cale Region: Artificial Intelligence Approach Application. Soil Science Society of America Journal, 2018, 82, 772-782.	2.2	10
119	Thallium in flowering cabbage and lettuce: Potential health risks for local residents of the Pearl River Delta, South China. Environmental Pollution, 2018, 241, 626-635.	7.5	26
120	Selenium reduces cadmium uptake into rice suspension cells by regulating the expression of lignin synthesis and cadmium-related genes. Science of the Total Environment, 2018, 644, 602-610.	8.0	117
121	Pentachlorophenol dissipation and ferrous iron accumulation in flooded paddy soils with contrasting organic matter contents and incorporation of legume green manures. Journal of Soils and Sediments, 2018, 18, 2463-2475.	3.0	2
122	Aqueous Fe(II)-Induced Phase Transformation of Ferrihydrite Coupled Adsorption/Immobilization of Rare Earth Elements. Minerals (Basel, Switzerland), 2018, 8, 357.	2.0	13
123	Microbial iron reduction as a method for immobilization of a low concentration of dissolved cadmium. Journal of Environmental Management, 2018, 217, 747-753.	7.8	20
124	Rapid Redox Processes of <i>c</i> â€Type Cytochromes in A Living Cell Suspension of <i>Shewanella oneidensis</i> MRâ€1. ChemistrySelect, 2017, 2, 1008-1012.	1.5	14
125	In situ spectral kinetics of quinone reduction by c-type cytochromes in intact Shewanella oneidensis MR-1 cells. Colloids and Surfaces A: Physicochemical and Engineering Aspects, 2017, 520, 505-513.	4.7	11
126	Arsenic mobility and bioavailability in paddy soil under iron compound amendments at different growth stages of rice. Environmental Pollution, 2017, 224, 136-147.	7.5	128

#	Article	IF	CITATIONS
127	Changes in the microbial community during repeated anaerobic microbial dechlorination of pentachlorophenol. Biodegradation, 2017, 28, 219-230.	3.0	10
128	Production of Hydrogen Peroxide in Groundwater at Rifle, Colorado. Environmental Science & Technology, 2017, 51, 7881-7891.	10.0	54
129	Silica nanoparticles alleviate cadmium toxicity in rice cells: Mechanisms and size effects. Environmental Pollution, 2017, 228, 363-369.	7.5	257
130	Exploring spatially varying and scale-dependent relationships between soil contamination and landscape patterns using geographically weighted regression. Applied Geography, 2017, 82, 101-114.	3.7	57
131	Redox dynamics and equilibria of c-type cytochromes in the presence of Fe(II) under anoxic conditions: Insights into enzymatic iron oxidation. Chemical Geology, 2017, 468, 97-104.	3.3	13
132	Fe(II)/Cu(II) interaction on goethite stimulated by an iron-reducing bacteria Aeromonas Hydrophila HS01 under anaerobic conditions. Chemosphere, 2017, 187, 43-51.	8.2	6
133	Effects of Cd on reductive transformation of lepidocrocite by Shewanella oneidensis MR-1. Acta Geochimica, 2017, 36, 479-481.	1.7	1
134	Detoxification and immobilization of chromite ore processing residue in spinel-based glass-ceramic. Journal of Hazardous Materials, 2017, 321, 449-455.	12.4	51
135	A novel organotrophic nitrate-reducing Fe( <scp>ii</scp> )-oxidizing bacterium isolated from paddy soil and draft genome sequencing indicate its metabolic versatility. RSC Advances, 2017, 7, 56611-56620.	3.6	8
136	Microaerobic iron oxidation and carbon assimilation and associated microbial community in paddy soil. Acta Geochimica, 2017, 36, 502-505.	1.7	7
137	Effects of Incubation Conditions on Cr(VI) Reduction by c-type Cytochromes in Intact Shewanella oneidensis MR-1 Cells. Frontiers in Microbiology, 2016, 7, 746.	3.5	46
138	A humic substance analogue AQDS stimulates Geobacter sp. abundance and enhances pentachlorophenol transformation in a paddy soil. Chemosphere, 2016, 160, 141-148.	8.2	33
139	Double-Barrier mechanism for chromium immobilization: A quantitative study of crystallization and leachability. Journal of Hazardous Materials, 2016, 311, 246-253.	12.4	55
140	Dynamics of the microbial community and Fe(III)-reducing and dechlorinating microorganisms in response to pentachlorophenol transformation in paddy soil. Journal of Hazardous Materials, 2016, 312, 97-105.	12.4	26
141	The availabilities of arsenic and cadmium in rice paddy fields from a mining area: The role of soil extractable and plant silicon. Environmental Pollution, 2016, 215, 258-265.	7.5	138
142	Fe(II)-induced phase transformation of ferrihydrite: The inhibition effects and stabilization of divalent metal cations. Chemical Geology, 2016, 444, 110-119.	3.3	91
143	Iron Redox Cycling Coupled to Transformation and Immobilization of Heavy Metals: Implications for Paddy Rice Safety in the Red Soil of South China. Advances in Agronomy, 2016, 137, 279-317.	5.2	137
144	Fractionation characteristics of rare earth elements (REEs) linked with secondary Fe, Mn, and Al minerals in soils. Acta Geochimica, 2016, 35, 329-339.	1.7	45

#	Article	IF	CITATIONS
145	pH dependence of quinone-mediated extracellular electron transfer in a bioelectrochemical system. Electrochimica Acta, 2016, 213, 408-415.	5.2	29
146	Heavy metal contaminations in soil-rice system: source identification in relation to a sulfur-rich coal burning power plant in Northern Guangdong Province, China. Environmental Monitoring and Assessment, 2016, 188, 460.	2.7	38
147	In Situ Spectral Kinetics of Cr(VI) Reduction by c-Type Cytochromes in A Suspension of Living Shewanella putrefaciens 200. Scientific Reports, 2016, 6, 29592.	3.3	22
148	Cadmium availability in rice paddy fields from a mining area: The effects of soil properties highlighting iron fractions and pH value. Environmental Pollution, 2016, 209, 38-45.	7.5	247
149	Enhanced visible-light photocatalytic activity of a TiO2 hydrosol assisted by H2O2: Surface complexation and kinetic modeling. Journal of Molecular Catalysis A, 2016, 414, 122-129.	4.8	22
150	Changes in the composition and diversity of microbial communities during anaerobic nitrate reduction and Fe(II) oxidation at circumneutral pH in paddy soil. Soil Biology and Biochemistry, 2016, 94, 70-79.	8.8	134
151	The diversity and abundance of As(III) oxidizers on root iron plaque is critical for arsenic bioavailability to rice. Scientific Reports, 2015, 5, 13611.	3.3	55
152	Burkholderiales participating in pentachlorophenol biodegradation in iron-reducing paddy soil as identified by stable isotope probing. Environmental Sciences: Processes and Impacts, 2015, 17, 1282-1289.	3.5	16
153	Arsenic availability in rice from a mining area: Is amorphous iron oxide-bound arsenic a source or sink?. Environmental Pollution, 2015, 199, 95-101.	7.5	131
154	Effects of landscape heterogeneity on the elevated trace metal concentrations in agricultural soils at multiple scales in the Pearl River Delta, South China. Environmental Pollution, 2015, 206, 264-274.	7.5	26
155	Rice husk based porous carbon loaded with silver nanoparticles by a simple and cost-effective approach and their antibacterial activity. Journal of Colloid and Interface Science, 2015, 455, 117-124.	9.4	44
156	The key microorganisms for anaerobic degradation of pentachlorophenol in paddy soil as revealed by stable isotope probing. Journal of Hazardous Materials, 2015, 298, 252-260.	12.4	39
157	Pyrosequencing revealed highly microbial phylogenetic diversity in ferromanganese nodules from farmland. Environmental Sciences: Processes and Impacts, 2015, 17, 213-224.	3.5	6
158	Using ensemble models to identify and apportion heavy metal pollution sources in agricultural soils on a local scale. Environmental Pollution, 2015, 206, 227-235.	7.5	123
159	Anaerobic degradation of Polychlorinated Biphenyls (PCBs) and Polychlorinated Biphenyls Ethers (PBDEs), and microbial community dynamics of electronic waste-contaminated soil. Science of the Total Environment, 2015, 502, 426-433.	8.0	73
160	Effects of nanoscale silica sol foliar application on arsenic uptake, distribution and oxidative damage defense in rice (Oryza sativa L.) under arsenic stress. RSC Advances, 2014, 4, 57227-57234.	3.6	54
161	Evaluating oxidation–reduction properties of dissolved organic matter from Chinese milk vetch ( <i>Astragalus sinicus</i> L.): a comprehensive multi-parametric study. Environmental Technology (United Kingdom), 2014, 35, 1916-1927.	2.2	7
162	Depassivation of Aged Fe <sup>0</sup> by Divalent Cations: Correlation between Contaminant Degradation and Surface Complexation Constants. Environmental Science & Technology, 2014, 48, 14564-14571.	10.0	61

#	Article	IF	CITATIONS
163	Iron Reduction Coupled to Reductive Dechlorination in Red Soil. Soil Science, 2014, 179, 457-467.	0.9	20
164	Reductions of Fe(III) and pentachlorophenol linked with geochemical properties of soils from Pearl River Delta. Geoderma, 2014, 217-218, 201-211.	5.1	15
165	Profiles, sources, and transport of polycyclic aromatic hydrocarbons in soils affected by electronic waste recycling in Longtang, south China. Environmental Monitoring and Assessment, 2014, 186, 3351-3364.	2.7	22
166	Accumulation of heavy metals in leaf vegetables from agricultural soils and associated potential health risks in the Pearl River Delta, South China. Environmental Monitoring and Assessment, 2014, 186, 1547-1560.	2.7	305
167	Competitive reduction of nitrate and iron oxides by Shewanella putrefaciens 200 under anoxic conditions. Colloids and Surfaces A: Physicochemical and Engineering Aspects, 2014, 445, 97-104.	4.7	25
168	Correlations between soil geochemical properties and Fe(III) reduction suggest microbial reducibility of iron in different soils from Southern China. Catena, 2014, 123, 176-187.	5.0	8
169	Influence of geochemical properties and land-use types on the microbial reduction of Fe(iii) in subtropical soils. Environmental Sciences: Processes and Impacts, 2014, 16, 1938-1947.	3.5	2
170	Heavy metal accumulation in balsam pear and cowpea related to the geochemical factors of variable-charge soils in the Pearl River Delta, South China. Environmental Sciences: Processes and Impacts, 2014, 16, 1790-1798.	3.5	11
171	2-Nitrophenol reduction promoted by S. putrefaciens 200 and biogenic ferrous iron: The role of different size-fractions of dissolved organic matter. Journal of Hazardous Materials, 2014, 279, 436-443.	12.4	25
172	Exogenous Electron Shuttle-Mediated Extracellular Electron Transfer of <i>Shewanella putrefaciens</i> 200: Electrochemical Parameters and Thermodynamics. Environmental Science & Technology, 2014, 48, 9306-9314.	10.0	85
173	The effect of ammonium chloride and urea application on soil bacterial communities closely related to the reductive transformation of pentachlorophenol. Journal of Hazardous Materials, 2014, 272, 10-19.	12.4	18
174	Arsenite oxidation and removal driven by a bio-electro-Fenton process under neutral pH conditions. Journal of Hazardous Materials, 2014, 275, 200-209.	12.4	94
175	Effect of nitrate addition on reductive transformation of pentachlorophenol in paddy soil in relation to iron(III) reduction. Journal of Environmental Management, 2014, 132, 42-48.	7.8	35
176	Fe(III) oxides accelerate microbial nitrate reduction and electricity generation by Klebsiella pneumoniae L17. Journal of Colloid and Interface Science, 2014, 423, 25-32.	9.4	48
177	Kinetics of Competitive Reduction of Nitrate and Iron Oxides by <i>Aeromonas hydrophila</i> HS01. Soil Science Society of America Journal, 2014, 78, 1903-1912.	2.2	16
178	Assessment of organochlorine pesticide contamination in relation to soil properties in the Pearl River Delta, China. Science of the Total Environment, 2013, 447, 160-168.	8.0	57
179	Depassivation of Aged Fe <sup>0</sup> by Ferrous Ions: Implications to Contaminant Degradation. Environmental Science & Technology, 2013, 47, 13712-13720.	10.0	64
180	Molecular weight-dependent electron transfer capacities of dissolved organic matter derived from sewage sludge compost. Journal of Soils and Sediments, 2013, 13, 56-63.	3.0	21

#	Article	IF	CITATIONS
181	Decolorization of Orange I under alkaline and anaerobic conditions by a newly isolated humus-reducing bacterium, Planococcus sp. MC01. International Biodeterioration and Biodegradation, 2013, 83, 17-24.	3.9	15
182	Fe(II)/Cu(II) interaction on α-FeOOH, kaolin and TiO2 for interfacial reactions of 2-nitrophenol reductive transformation. Colloids and Surfaces A: Physicochemical and Engineering Aspects, 2013, 425, 92-98.	4.7	15
183	Effects of dissolved organic matter on adsorbed Fe(II) reactivity for the reduction of 2-nitrophenol in TiO2 suspensions. Chemosphere, 2013, 93, 29-34.	8.2	30
184	Association between ferrous iron accumulation and pentachlorophenol degradation at the paddy soil–water interface in the presence of exogenous low-molecular-weight dissolved organic carbon. Chemosphere, 2013, 91, 1547-1555.	8.2	32
185	Electron transfer capacity dependence of quinone-mediated Fe(III) reduction and current generation by Klebsiella pneumoniae L17. Chemosphere, 2013, 92, 218-224.	8.2	68
186	Anaerobic Transformation of DDT Related to Iron(III) Reduction and Microbial Community Structure in Paddy Soils. Journal of Agricultural and Food Chemistry, 2013, 61, 2224-2233.	5.2	47
187	Depassivation of Aged Fe <sup>0</sup> by Inorganic Salts: Implications to Contaminant Degradation in Seawater. Environmental Science & amp; Technology, 2013, 47, 7350-7356.	10.0	41
188	Bio-current as an indicator for biogenic Fe(II) generation driven by dissimilatory iron reducing bacteria. Biosensors and Bioelectronics, 2013, 39, 51-56.	10.1	34
189	Humic substanceâ€mediated reduction of iron( <scp>III</scp> ) oxides and degradation of 2,4â€ <scp>D</scp> by an alkaliphilic bacterium, <i><scp>C</scp>orynebacterium humireducens</i> â€ <scp>MFC</scp> â€5. Microbial Biotechnology, 2013, 6, 141-149.	4.2	34
190	Heterogeneous Nucleophilic Transformation of Metolachlor by Bisulfide on Alumina Surface. Clean - Soil, Air, Water, 2013, 41, 856-864.	1.1	4
191	Dependence of the electron transfer capacity on the kinetics of quinone-mediated Fe( <scp>iii</scp> ) reduction by two iron/humic reducing bacteria. RSC Advances, 2013, 4, 2284-2290.	3.6	36
192	Effect of pH and Weathering Indices on the Reductive Transformation of 2-Nitrophenol in South China. Soil Science Society of America Journal, 2012, 76, 1579-1591.	2.2	17
193	Phytoextraction of Pb and Cu Contaminated Soil With Maize and Microencapsulated EDTA. International Journal of Phytoremediation, 2012, 14, 727-740.	3.1	22
194	Biostimulation of Indigenous Microbial Communities for Anaerobic Transformation of Pentachlorophenol in Paddy Soils of Southern China. Journal of Agricultural and Food Chemistry, 2012, 60, 2967-2975.	5.2	62
195	Enhancement effect of two ecological earthworm species (Eisenia foetida and Amynthas robustus E.) Tj ETQq1 1 2012, 14, 1551.	0.784314 2.1	rgBT /Oved 27
196	Effects of the Fe <sup>II</sup> /Cu <sup>II</sup> Interaction on Copper Aging Enhancement and Pentachlorophenol Reductive Transformation in Paddy Soil. Journal of Agricultural and Food Chemistry, 2012, 60, 630-638.	5.2	24
197	Electrochemical evidence of Fe(II)/Cu(II) interaction on titanium oxide for 2-nitrophenol reductive transformation. Applied Clay Science, 2012, 64, 84-89.	5.2	12
198	Dechlorinating transformation of propachlor through nucleophilic substitution by dithionite on the surface of alumina. Journal of Soils and Sediments, 2012, 12, 724-733.	3.0	127

#	Article	IF	CITATIONS
199	Effects of calcium peroxide on arsenic uptake by celery (Apium graveolens L.) grown in arsenic contaminated soil. Chemosphere, 2012, 86, 1106-1111.	8.2	23
200	Reduction of structural Fe(III) in oxyhydroxides by Shewanella decolorationis S12 and characterization of the surface properties of iron minerals. Journal of Soils and Sediments, 2012, 12, 217-227.	3.0	66
201	Enhanced nitrate reduction and current generation by Bacillus sp. in the presence of iron oxides. Journal of Soils and Sediments, 2012, 12, 354-365.	3.0	42
202	Comparison of Aqueous Photoreactions with TiO <sub>2</sub> in its Hydrosol Solution and Powdery Suspension for Light Utilization. Industrial & Engineering Chemistry Research, 2011, 50, 7841-7848.	3.7	17
203	Heavy metal contamination in soils and vegetables near an e-waste processing site, south China. Journal of Hazardous Materials, 2011, 186, 481-490.	12.4	565
204	A rapid and simple electrochemical method for evaluating the electron transfer capacities of dissolved organic matter. Journal of Soils and Sediments, 2011, 11, 467-473.	3.0	56
205	Anaerobic degradation of phenanthrene by a newly isolated humus-reducing bacterium, Pseudomonas aeruginosa strain PAH-1. Journal of Soils and Sediments, 2011, 11, 923-929.	3.0	31
206	Effect of pH on pentachlorophenol degradation in irradiated iron/oxalate systems. Chemical Engineering Journal, 2011, 168, 1209-1216.	12.7	34
207	Understanding the role of Fe(III)/Fe(II) couple in mediating reductive transformation of 2-nitrophenol in microbial fuel cells. Bioresource Technology, 2011, 102, 1131-1136.	9.6	18
208	Reduction of iron oxides by Klebsiella pneumoniae L17: Kinetics and surface properties. Colloids and Surfaces A: Physicochemical and Engineering Aspects, 2011, 379, 143-150.	4.7	23
209	Reductive Activity of Adsorbed Fe(II) on Iron (Oxyhydr)Oxides for 2-Nitrophenol Transformation. Clays and Clay Minerals, 2010, 58, 682-690.	1.3	19
210	Comparison of dissolved organic matter from sewage sludge and sludge compost as electron shuttles for enhancing Fe(III) bioreduction. Journal of Soils and Sediments, 2010, 10, 722-729.	3.0	30
211	Arsenic contamination and potential health risk implications at an abandoned tungsten mine, southern China. Environmental Pollution, 2010, 158, 820-826.	7.5	208
212	The oxidative transformation of sodium arsenite at the interface of α-MnO2 and water. Journal of Hazardous Materials, 2010, 173, 675-681.	12.4	82
213	Heterogeneous photodegradation of pentachlorophenol and iron cycling with goethite, hematite and oxalate under UVA illumination. Journal of Hazardous Materials, 2010, 174, 64-70.	12.4	62
214	A dual-chamber microbial fuel cell with conductive film-modified anode and cathode and its application for the neutral electro-Fenton process. Electrochimica Acta, 2010, 55, 2048-2054.	5.2	119
215	Enhanced photocatalytic activity of Ce3+-TiO2 hydrosols in aqueous and gaseous phases. Chemical Engineering Journal, 2010, 157, 475-482.	12.7	44
216	A polypyrrole/anthraquinone-2,6-disulphonic disodium salt (PPy/AQDS)-modified anode to improve performance of microbial fuel cells. Biosensors and Bioelectronics, 2010, 25, 1516-1520.	10.1	189

#	Article	IF	CITATIONS
217	Fe(III)-enhanced anaerobic transformation of 2,4-dichlorophenoxyacetic acid by an iron-reducing bacterium Comamonas koreensis CY01. FEMS Microbiology Ecology, 2010, 71, 106-113.	2.7	62
218	Development of a Photocatalytic Wet Scrubbing Process for Gaseous Odor Treatment. Industrial & amp; Engineering Chemistry Research, 2010, 49, 3617-3622.	3.7	21
219	Bio-Electro-Fenton Process Driven by Microbial Fuel Cell for Wastewater Treatment. Environmental Science & Technology, 2010, 44, 1875-1880.	10.0	223
220	Microbial biomass, enzyme and mineralization activity in relation to soil organic C, N and P turnover influenced by acid metal stress. Soil Biology and Biochemistry, 2009, 41, 969-977.	8.8	161
221	Interactively interfacial reaction of iron-reducing bacterium and goethite for reductive dechlorination of chlorinated organic compounds. Science Bulletin, 2009, 54, 2800-2804.	9.0	14
222	Microbial fuel cell with an azo-dye-feeding cathode. Applied Microbiology and Biotechnology, 2009, 85, 175-183.	3.6	114
223	Foliar application of two silica sols reduced cadmium accumulation in rice grains. Journal of Hazardous Materials, 2009, 161, 1466-1472.	12.4	149
224	Electrochemical Evidences for Promoted Interfacial Reactions: The Role of Fe(II) Adsorbed onto γ-Al <sub>2</sub> O <sub>3</sub> and TiO <sub>2</sub> in Reductive Transformation of 2-Nitrophenol. Environmental Science & Technology, 2009, 43, 3656-3661.	10.0	38
225	Reductive transformation of 2-nitrophenol by Fe(II) species in Î <sup>3</sup> -aluminum oxide suspension. Applied Clay Science, 2009, 46, 95-101.	5.2	13
226	Dependence of Sulfadiazine Oxidative Degradation on Physicochemical Properties of Manganese Dioxides. Industrial & Engineering Chemistry Research, 2009, 48, 10408-10413.	3.7	53
227	The concentrations, distribution and sources of PAHs in agricultural soils and vegetables from Shunde, Guangdong, China. Environmental Monitoring and Assessment, 2008, 139, 61-76.	2.7	89
228	Enhancement of the reductive transformation of pentachlorophenol by polycarboxylic acids at the iron oxide–water interface. Journal of Colloid and Interface Science, 2008, 321, 332-341.	9.4	70
229	TiO2 hydrosols with high activity for photocatalytic degradation of formaldehyde in a gaseous phase. Journal of Hazardous Materials, 2008, 152, 347-355.	12.4	87
230	Photodegradation of 2-mercaptobenzothiazole in the Î <sup>3</sup> -Fe2O3/oxalate suspension under UVA light irradiation. Journal of Hazardous Materials, 2008, 153, 426-433.	12.4	68
231	The oxidative degradation of 2-mercaptobenzothiazole at the interface of β-MnO2 and water. Journal of Hazardous Materials, 2008, 154, 1098-1105.	12.4	46
232	Effects of peptizing conditions on nanometer properties and photocatalytic activity of TiO2 hydrosols prepared by H2TiO3. Journal of Hazardous Materials, 2008, 155, 90-99.	12.4	23
233	The enhancement of adsorption and photocatalytic activity of rare earth ions doped TiO2 for the degradation of Orange I. Dyes and Pigments, 2008, 76, 477-484.	3.7	129
234	Heterogeneous Photodegradation of Pentachlorophenol with Maghemite and Oxalate under UV Illumination. Environmental Science & Technology, 2008, 42, 7918-7923.	10.0	85

#	Article	IF	CITATIONS
235	Occurrence of phthalate esters in water and sediment of urban lakes in a subtropical city, Guangzhou, South China. Environment International, 2008, 34, 372-380.	10.0	210
236	Reductive transformation of pentachlorophenol on the interface of subtropical soil colloids and water. Geoderma, 2008, 148, 70-78.	5.1	34
237	AgNO <sub>3</sub> -Induced Photocatalytic Degradation of Odorous Methyl Mercaptan in Gaseous Phase: Mechanism of Chemisorption and Photocatalytic Reaction. Environmental Science & Technology, 2008, 42, 4540-4545.	10.0	47
238	Pollution assessment, distribution and sources of PAHs in agricultural soils of Pearl River Delta—The biggest manufacturing Base in China. Journal of Environmental Science and Health - Part A Toxic/Hazardous Substances and Environmental Engineering, 2007, 42, 1979-1987.	1.7	21
239	The effect of substituent groups on the reductive degradation of azo dyes by zerovalent iron. Journal of Hazardous Materials, 2007, 145, 305-314.	12.4	99
240	Effect of alumina on photocatalytic activity of iron oxides for bisphenol A degradation. Journal of Hazardous Materials, 2007, 149, 199-207.	12.4	94
241	Heterogeneous photodegradation of bisphenol A with iron oxides and oxalate in aqueous solution. Journal of Colloid and Interface Science, 2007, 311, 481-490.	9.4	112
242	The effect of iron oxides and oxalate on the photodegradation of 2-mercaptobenzothiazole. Journal of Molecular Catalysis A, 2006, 252, 40-48.	4.8	81
243	Photodegradation of orange I in the heterogeneous iron oxide–oxalate complex system under UVA irradiation. Journal of Hazardous Materials, 2006, 137, 1016-1024.	12.4	70
244	The effect of erbium on the adsorption and photodegradation of orange I in aqueous Er3+-TiO2 suspension. Journal of Hazardous Materials, 2006, 138, 471-478.	12.4	72
245	Effect of iron oxides and carboxylic acids on photochemical degradation of bisphenol A. Biology and Fertility of Soils, 2006, 42, 409-417.	4.3	29
246	Spatial distribution of heavy metals of agricultural soils in Dongguan, China. Journal of Environmental Sciences, 2004, 16, 912-8.	6.1	7